Exploiting quantum parallelism of entanglement for a complete experimental quantum characterization of a single-qubit device

Francesco De Martini,* Andrea Mazzei,† and Marco Ricci‡
Istituto Nazionale per la Fisica della Materia, Dipartimento di Fisica, Università "La Sapienza," Roma 00185, Italy§

Giacomo Mauro D'Ariano‖
Quantum Optics and Information Group, Istituto Nazionale di Fisica della Materia, Unità di Pavia¶ *and Dipartimento di Fisica "A. Volta," via Bassi 6, I-27100 Pavia, Italy*

(Received 7 August 2002; published 24 June 2003)

We present the full experimental quantum tomographic characterization of a single-qubit device achieved with a single entangled input state. The entangled input state plays the role of all possible input states in quantum parallel on the tested device. The method can be trivially extended to any *n*-qubit device by just replicating the whole experimental setup *n* times.

DOI: 10.1103/PhysRevA.67.062307 PACS number(s): 03.67.Lx, 03.65.Wj, 03.65.Ud, 42.50.Dv

The new field of quantum information [1] has recently opened the way to realize radically new processing devices, with the possibility of tremendous speedups of complex computational tasks, and of cryptographic communications guaranteed by the laws of physics. Among the many problems posed by the new information technology, there is the need of making a complete experimental characterization of the functioning of the new quantum devices. As shown recently in Ref. [2], quantum mechanics provides us with the perfect tool to achieve the task easily and efficiently: this is the so-called *quantum entanglement*, the basis of the quantum parallelism of future computers. In this paper, we present the full experimental quantum characterization of a single-qubit device, based on this method. Since the method can be easily extended to any *n*-qubit device, the present experiment represents a test of the feasibility and of the experimental limits of the new general tomographic method.

How we characterize the operation of a device? In quantum mechanics, the evolution of the state is completely described by the so-called *quantum operation* [3] of the device, which here we will denote by E. More precisely, the output state ρ_{out} is given by the quantum operation E applied to the input state ρ_{in} as follows

$$\rho_{out}=\frac{E(\rho_{in})}{\mathrm{Tr}[E(\rho_{in})]}. \tag{1}$$

The normalization constant $\mathrm{Tr}[E(\rho_{in})]$ in Eq. (1) is also the probability of occurrence of the transformation E (e.g., when there are other possible alternatives, such as when we consider the state transformation due to a measuring device for a given outcome). Therefore, apart from a normalization factor, the quantum evolution is always linear, with the quantum operation playing the role of the so-called *transfer matrix* of the device, a mathematical tool very popular in optics and electrical engineering.

Now the problem is: how to reconstruct the form of E experimentally? Since E is essentially a transfer matrix for a linear system, one would be tempted to adopt the conventional method of running an *orthogonal basis* $|n\rangle$ of inputs and measuring the corresponding outputs by *quantum tomography* [4]. However, since states are actually operators—not vectors—as a consequence of the polarization identity in order to get all off-diagonal (complex) matrix elements of the state, one actually needs to run not the basis itself, but all the linear combinations of its vectors $2^{-1/2}(|n'\rangle+\kappa|n''\rangle)$, with $\kappa=\pm 1,\pm i$. In the following we will call such sets of states *faithful*, since they are sufficient to make a complete tomography of a quantum operation. This method is essentially the *quantum process tomography* given in Ref. [1], which was experimentally demonstrated in nuclear-magnetic resonance NMR [5] and recently in quantum optics [6]. The main problem with such method is the fact that in most practical situations, faithful sets of input states are not feasible in the lab. For example, for continuous-variables process tomography in the Fock representation, the states $|n'\rangle$ and $|n''\rangle$ would be photon number states, and achieving their superpositions will remain a dream for experimentalists for many years. But here the *quantum parallelism* of entanglement comes to help us, with a single-input entangled state that is equivalent to running all possible input states in parallel [2]. Thus, we do not need to prepare a complete set of states, but just a single entangled one, a state commonly available in any modern quantum optical laboratory.

In the following, we will use the double-ket notation $|\Psi\rangle\rangle\in\mathcal{H}\otimes\mathcal{H}$ to denote bipartite states corresponding to the matrix Ψ_{nm} of coefficients on fixed given orthonormal basis $|n\rangle\otimes|m\rangle\equiv|nm\rangle$ of $\mathcal{H}\otimes\mathcal{H}$,

$$|\Psi\rangle\rangle=\sum_{nm}\Psi_{nm}|nm\rangle. \tag{2}$$

*Electronic address: francesco.demartini@uniroma1.it
†Electronic address: andrea.mazzei@uniroma1.it
‡Electronic address: marco.ricci@uniroma1.it
§URL: http://quantumoptics.phys.uniroma1.it
‖Also at Department of Electrical and Computer Engineering, Northwestern University, Evanston, IL 60208. Electronic address: dariano@unipv.it
¶URL: http://www.qubit.it

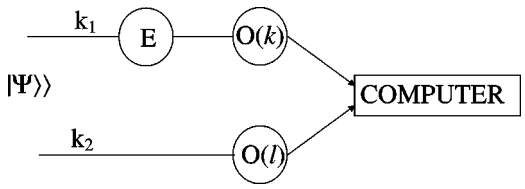

FIG. 1. General experimental scheme of the method for the tomographic estimation of the quantum operation E of a single-qubit device. Two identical quantum systems—two optical beams in the present experiment—are prepared in an entangled state $|\Psi\rangle\rangle$. One of the two systems undergoes the quantum operation E, whereas the other is left untouched. At the output one makes a quantum tomographic estimation, by measuring jointly two observables (each for each beam) from a *quorum* $\{Q(l)\}$. In the present experiment, the quorum is represented by the set of Pauli operators σ_x, σ_y, and σ_z.

In our optical implementation the entangled systems consist of two single-mode optical beams, and the Hilbert space is two dimensional, since we will consider only single-photon polarization states. The key feature of the method implies that only one of the two systems is an input into the *unknown* transformation E, whereas the other is left untouched, as in Fig. 1. This setup leads to the output state R_{out}, which in tensor notation writes as follows:

$$R_{out}=E\otimes I(|\Psi\rangle\rangle\langle\langle\Psi|), \tag{3}$$

where I denotes the identical operation. It is a result of linear algebra that R_{out} is in one-to-one correspondence with the quantum operation E, as long as the state $|\Psi\rangle\rangle$ is *full rank*, i.e., its matrix Ψ is invertible. This is the case of a so-called *maximally entangled* state, where the matrix Ψ is proportional to a unitary one. Full-rank entangled states can be easily generated by spontaneous parametric down-conversion of vacuum, as in the experiment reported here. Note that even when a faithful set of input states is available in the lab—which is actually true in our case of single-photon-polarization states—nevertheless, a single faithful entangled state can be much more efficient and more practical. As a matter of fact, in practice, generation of single-photon-polarization states relies anyway on entanglement, and, as we will see in the following, the present method uses all experimental data much more efficiently than the conventional quantum process tomography [1,6].

Now, how to characterize the entangled state R_{out} at the output? For this purpose, a technique for the full determination of the quantum state has been introduced and developed since 1994. The method named quantum tomography [4] has been initially introduced for the state of a single mode of radiation, the so-called *homodyne tomography*, and thereafter it has been generalized to any quantum system. The basis of the method is the measurement of a suitably complete set of observables called *quorum*. In our case, we need to measure jointly two quora of observables on the entangled qubit, here the quorum being the Pauli matrices σ_x, σ_y, σ_z. The qubit is encoded on polarization of single photons as follows:

$$|0\rangle\doteq h^\dagger|\Omega\rangle, \quad |1\rangle\doteq v^\dagger|\Omega\rangle, \tag{4}$$

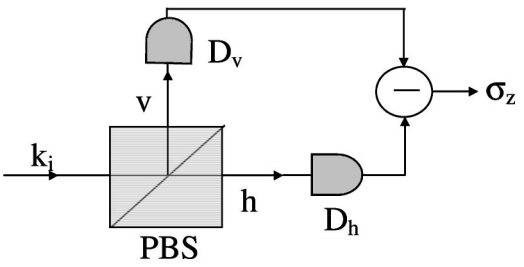

FIG. 2. Pauli-matrix σ_z measurement apparatus for photon-polarization qubits inserted at the end of each optical beam. The beam is split by a polarizing beam splitter (PBS) into its horizontal and vertical components, which are separately detected and recorded with a plus and minus sign, respectively. For measuring the other two Pauli matrices σ_x and σ_y, the PBS is preceded by a suitably oriented $\lambda/2$ and $\lambda/4$ wave plate, respectively (see text).

where $|\Omega\rangle$ denotes the electromagnetic vacuum, and h, $h^\dagger$ and v, $v^\dagger$ the annihilation and creation operators of the horizontally and vertically polarized modes associated with a fixed wave vector $\mathbf{k}$, respectively. In synthesis, Eq. (4) means that the ''logical zero'' is encoded on a single horizontally polarized photon, whereas the ''logical one'' is encoded on a vertically polarized photon. In the present representation, the Pauli matrices are written as follows:

$$\sigma_x=h^\dagger v+v^\dagger h, \quad \sigma_y=i(h^\dagger v-v^\dagger h), \quad \sigma_z=h^\dagger h-v^\dagger v. \tag{5}$$

According to Eq. (5), the σ_z photodetector is simply achieved as in Fig. 2.

In order to understand how to design detectors for σ_y and σ_x, we still need some simple algebra for wave plates. The ring of Pauli matrices is completed by including the ''identity'' $\sigma_0=h^\dagger h+v^\dagger v$, corresponding to single-photon states. In the following, we use the popular relativistic conventions, denoting by $\vec{\sigma}$ the three-vector of operators $\vec{\sigma}=(\sigma_1,\sigma_2,\sigma_3)$ and by σ the four-vector $\sigma=(\sigma_0,\sigma_1,\sigma_2,\sigma_3)$, and use Greek indices for three-vector components $\alpha=1,2,3$ (or $\alpha=x,y,z$), and Latin indices for four-vector components $i=0,1,2,3$.

A wave plate changes the two radiation modes according to the matrix transformation

$$\begin{bmatrix} h \\ v \end{bmatrix} \to \mathbb{W}_{\phi,\theta}\begin{bmatrix} h \\ v \end{bmatrix}, \tag{6}$$

where the matrix $\mathbb{W}_{\phi,\theta}$ is given by

$$\mathbb{W}_{\phi,\theta}=\begin{bmatrix} z_+ + cz_- & sz_- \\ sz_- & z_+ - cz_- \end{bmatrix}, \tag{7}$$

where $s=\sin 2\theta$, $c=\cos 2\theta$, $z_\pm=\frac{1}{2}(1\pm e^{i\phi})$, θ is the wave-plate orientation angle around the wave vector $\mathbf{k}$, $\phi=2\pi\delta/\lambda$, λ is the wave length, and δ is the length of the optical path through the plate. Special cases are the $\lambda/4$ wave plate that can be used with $\theta=\pi/4$ to give the right c_+ and left c_- circularly polarized modes $c_\pm=e^{i\pi/4}2^{-1/2}(\pm h+iv)$, and the $\lambda/2$ wave plate that can be used to give the

diagonal linearly polarized modes $d_{\pm}=2^{-1/2}(h\pm v)$. On the Pauli operator vector $\vec{\sigma}$, the mode transformation due to a wave plate is

$$\vec{\sigma}\rightarrow\mathbb{R}_{\phi,\theta}\vec{\sigma}, \tag{8}$$

with rotation matrix

$$\mathbb{R}_{\phi,\theta}=\begin{bmatrix} s^2+c^2\cos\phi & -c\cos\phi & sc(1-\cos\phi) \\ c\sin\phi & \cos\phi & -s\sin\phi \\ sc(1-\cos\phi) & s\sin\phi & c^2+s^2\cos\phi \end{bmatrix}. \tag{9}$$

From Eq. (9) we can see that a σ_x detector can be obtained by preceding the σ_z detector with a $\lambda/2$ wave plate oriented at $\theta=\pi/8$, whereas a σ_y detector is obtained by preceding the σ_z detector with a $\lambda/4$ wave plate oriented at $\theta=\pi/4$. When collecting data at a σ_α detector, we will denote by $s_\alpha=\pm1$ the corresponding random outcome, $s_\alpha=+1$ corresponding to the h-detector flashing, and $s_\alpha=-1$ to the v-detector flashing. The general experimental setup is then given by two Pauli detectors—for measuring σ_α and σ_β for varying α and β –at the output of the entangled beams, as in Fig. 1. The experimental data are collected in coincidence, with two of the four photodetector firings, one for each Pauli detector, thus guaranteeing that the result will be essentially unaffected by quantum efficiency. The experimental correlations $\overline{s_i^{(1)}s_j^{(2)}}$ of the random outcomes $s_i^{(n)}$ of the detector at the nth beam ($n=1,2$) on the entangled state $|\Psi\rangle\rangle$ must coincide with the following theoretical expectations:

$$\overline{s_i^{(1)}s_j^{(2)}}=\langle\langle\Psi|(\sigma_i^{(1)}\otimes\sigma_j^{(2)})|\Psi\rangle\rangle=\mathrm{Tr}[\Psi^+\sigma_i\Psi\sigma_j^*], \tag{10}$$

and, obviously, $\overline{s_i^{(1)}}\equiv\overline{s_i^{(1)}s_0^{(2)}}$ and $\overline{s_i^{(2)}}\equiv\overline{s_0^{(1)}s_i^{(2)}}$. For maximally entangled states we have the isotropy condition $\overline{s_\alpha^{(1)}}=\overline{s_\alpha^{(2)}}=0$ for $\alpha=x,y,z$. The four Bell states will correspond to the four Pauli matrices σ_j via a state coefficients matrix Ψ given by $\Psi=(1/\sqrt{2})\sigma_j$. On the other hand, when a quantum device performing the unitary transformation U is inserted in one of the two entangled beams as in Fig. 1, the entangled state $|\Psi\rangle\rangle$ is changed to $U\otimes I|\Psi\rangle\rangle$, which corresponds to the new coefficients matrix $\Psi\rightarrow U\Psi$. In our laboratory we used the ''triplet'' state corresponding to $\Psi=\sigma_x/\sqrt{2}$, which is generated via spontaneous parametric down-conversion by an optical parametric amplifier physically consisting of a nonlinear BBO (ß-barium-borate) crystal plate, 1.5 mm thick, cut for type-II phase matching and excited by a pulsed mode-locked ultraviolet laser UV having pulse duration $\tau=140$ fsec and wavelength $\lambda_p=397.5$ nm. The wavelength of the emitted photons is $\lambda=795$ nm. The measurement apparatus consisted of two equal polarizing beam splitters with output modes coupled to four equal Si-avalanche photodetectors SPCM-AQR14 with quantum efficiencies QE$\simeq$0.42. The beams exciting the detectors are filtered by equal interference filters within a bandwidth $\Delta\lambda=3$ nm. The detector outputs are finally analyzed by a computer.

With the above apparatus, we want now to experimentally determine the matrix elements of the state $|\Psi\rangle\rangle$ in Eq. (2). From the trivial identity

$$\langle nm|\Psi\rangle\rangle=\Psi_{nm}, \tag{11}$$

we obtain the matrix Ψ_{nm} for the *input states* in terms of the following ensemble averages:

$$\Psi_{nm}=e^{i\varphi}\frac{\langle\langle\Psi|01\rangle\langle nm|\Psi\rangle\rangle}{\sqrt{\langle\langle\Psi|01\rangle\langle01|\Psi\rangle\rangle}}, \tag{12}$$

where $\exp(i\varphi)=\Psi_{01}/|\Psi_{01}|$ is an unmeasurable phase factor. The choice of the vector $|01\rangle$ is arbitrary, and it is needed only for the sake of normalization, e.g., we could have used $|10\rangle$ or $|11\rangle$, instead. Using the *tomographic expansion* over the four Pauli matrices [4], we see that, via Eq. (12), the matrix element of the input state is obtained from the following experimental averages:

$$\Psi_{nm}=\frac{1}{4\sqrt{p}}\sum_{ij}Q_{nm}^{ij}\overline{s_i^{(1)}s_j^{(2)}}, \tag{13}$$

where

$$p=\langle\langle\Psi|01\rangle\langle01|\Psi\rangle\rangle=\tfrac{1}{4}\overline{(1+s_3^{(1)})(1-s_3^{(2)})} \tag{14}$$

is the fraction of events with one σ_z-detector firing on h and the other on v, and the matrix Q_{nm}^{ij} is given by

$$Q_{nm}^{ij}=\langle n|\sigma_i|0\rangle\langle m|\sigma_j|1\rangle. \tag{15}$$

The unitary matrix U_{nm} of the device is now obtained with the same averaging as above, but now for the state at the output of the device $|U\Psi\rangle\rangle=(U\otimes I)|\Psi\rangle\rangle$, namely,

$$(U\Psi)_{nm}=e^{i\varphi}\frac{\langle\langle U\Psi|01\rangle\langle nm|\Psi U\rangle\rangle}{\sqrt{\langle\langle U\Psi|01\rangle\langle01|\Psi U\rangle\rangle}}, \tag{16}$$

where we use again Eqs. (14) and (15), but now the average expressed by Eq. (12) is carried out over the output state $|U\Psi\rangle\rangle$. The (complex) matrix elements U_{nm} are obtained from Eq. (16) by matrix inversion. This is, of course, possible since the matrix Ψ is invertible, due to the maximally entangled character of $|\Psi\rangle\rangle$.

An experimental demonstration of the tomographic method is given in Figs. 3 and 4, where both the *real* and *imaginary parts* of the four measured matrix elements of the unitary operator U of the analyzed device are reported for two different devices, and compared with the theoretical values. As an see, the experimental results are in very good agreement with theory, within experimental errors. As a first experimental demonstration we have considered only unitary devices, however, it is clear that the method works for nonunitary devices as well. It is also obvious that the method can be used to characterize n qubit devices—e.g., a controlled-

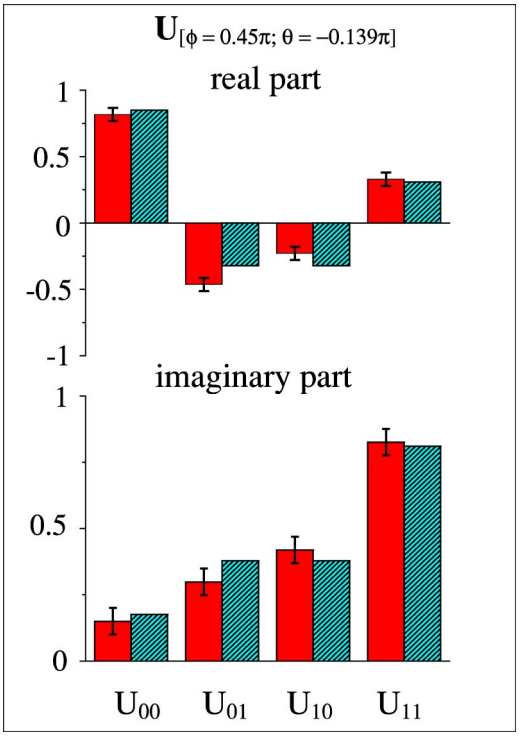

FIG. 3. Experimental characterization of a single optical wave plate with retardation phase $\phi = 0.45\pi$ and orientation angle of the optical axis with respect to the laboratory horizontal direction $\theta = -0.138\pi$. The experimental matrix elements U_{nm} of the wave plate are superimposed to statistical errors for 8000 events, and compared with the theoretical values.

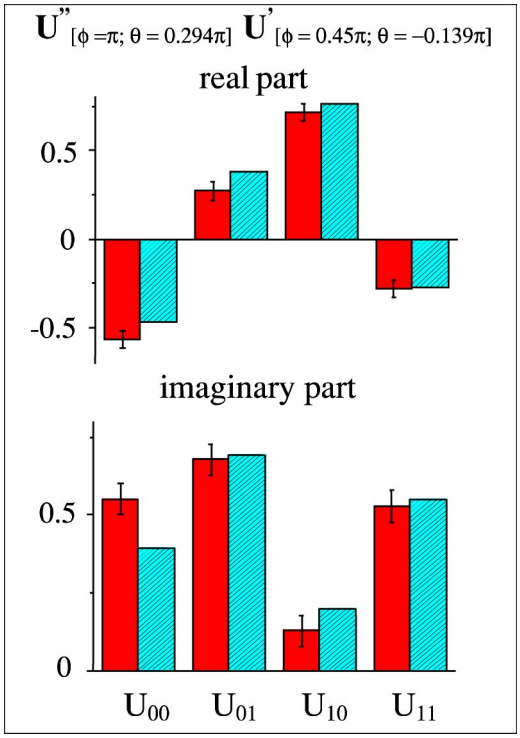

FIG. 4. The same experimental characterization as in Fig. 3, here for a device made of a series of two optical wave plates: a wave plate with $\phi = 0.45\pi$ and $\theta = -0.138\pi$ followed by another wave plate with $\phi = \pi$ and $\theta = +0.29\pi$.

NOT gate—in which case we just need to multiply by n the whole setup, by providing an input entangled state and two Pauli detectors for each qubit of the device, with the full quantum characterization of the device obtained by a joint tomography on all output entangled pairs. It is clear that the precision of the method will not depend on the particular tested device—whether it is unitary or not—and will also be independent of the number of qubits. What makes the method particularly reliable in the present single-photon-polarization encoding is the fact that all measurements are performed in coincidence, making the effect of nonunit quantum efficiency of detectors negligible, and effectively purifying the input entangled state. In a different context—e.g., for continuous variables, such as homodyne tomography of twin beams [7]—quantum efficiency and entanglement purity will actually affect the final result: however, the quantum tomographic reconstruction can handle all these kinds of detection noises below some thresholds [4], and a mixed input state in place of $|\Psi\rangle\rangle$ works well (but less efficiently) as long as the state is *faithful*, namely, it is related to a maximally entangled one by an invertible map [8]. Unfortunately, for the twin-beam homodyne tomography [7], faithfulness requires the knowledge of the phase of the pump relative to the local oscillator—a feasible but difficult experimental task—whereas in the present experiment the form of the entangled input state is completely under control, being determined only by the orientation of the nonlinear crystal with respect to the pump wave vector and polarization.

In conclusion, we have given the demonstration of a new tomographic method which allows us to perform a complete characterization of any quantum device, exploiting the intrinsic parallelism of quantum entanglement, with a single entangled state playing the role of all possible input states in quantum parallel. The method works for any generally nonunitary multiqubit device, and is particularly reliable in the present context of single-photon-polarization encoding of the qubit.

This work has been supported by the FET European Network on QIC (Contract No. IST-2000-29681-ATESIT) and the INFM Grant No. PRA 2001 CLON.

[1] I. L. Chuang and M. A. Nielsen, *Quantum Information and Quantum Computation* (Cambridge University Press, Cambridge, 2000).

[2] G.M. D'Ariano and P. Lo Presti, Phys. Rev. Lett. **86**, 4195 (2001).

[3] K. Kraus, *States, Effects, and Operations* (Springer-Verlag, Berlin, 1983).

[4] G. M. D'Ariano, in *Quantum Tomography*, Proceedings of the

International School ''Enrico Fermi,'' Varenna, edited by F. De Martini and C. Monroe (Editrice Compositori, Bologna, 2002).
[5] A.M. Childs, I.L. Chuang, and D.W. Leung, Phys. Rev. A **64**, 012314 (2001).
[6] P. Kwiat, in *Quantum Communication, Measurements and Computing (Cambridge QCMC'02)*, edited by J. Shapiro and O. Hirota (Rinton Press, Paramus, NJ, 2002).
[7] M. Vasilyev, S.-K. Choi, P. Kumar, and G.M. D'Ariano, Phys. Rev. Lett. **84**, 2354 (2000).
[8] G. M. D'Ariano and P. Lo Presti (unpublished).